

Paleomagnetic Tests of Pacific Plate Reconstructions and Implications for Motion Between Hotspots

Gary D. Acton* and Richard G. Gordon†

The plate-motion circuit through the South Pacific and Antarctica is shown to fail paleomagnetic tests of consistency. These failures imply that reconstructions of Pacific basin plates relative to surrounding plates inferred from this circuit are systematically in error and that estimates of motion between hotspots inferred from this circuit are probably too large. Therefore, the motions between hotspots remain poorly known and may be much smaller than previously estimated.

It would be surprising if there was no causal link between motions and tectonics across circum-Pacific margins. A prerequisite to establishing both the existence and an understanding of this link is an accurate set of reconstructions of the positions and displacements of the Pacific oceanic plates—which include the Pacific, Farallon, and Kula plates—relative to the circum-Pacific plates—which include the North American, Caribbean, South American, and Eurasian plates. Estimating these past displacements and velocities is more difficult than estimating the motions between plates in the Atlantic, where most plate pairs—for example, the North American and African plates—are separating along the Mid-Atlantic Ridge, which has preserved a record of the relative motions in the locations of fracture zones and magnetic-reversal isochrons in the Atlantic sea floor. In contrast, plate motions across circum-Pacific margins have been dominantly convergent, leaving no direct precise record of motions, except in the Gulf of California for the past few million years (My). Hence, indirect methods of inferring past plate displacements and velocities are required. Two main approaches have been used.

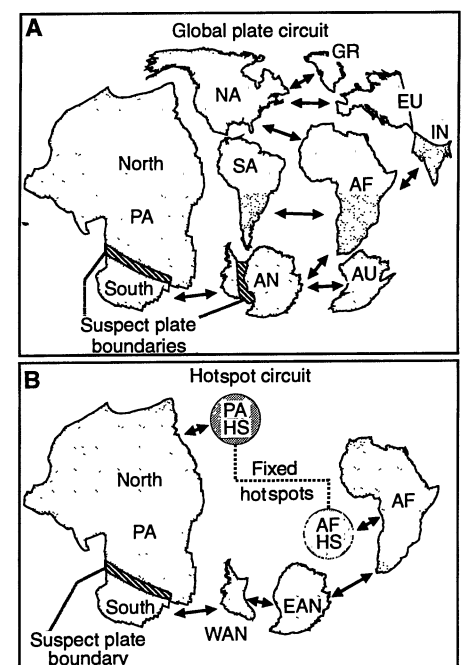
The first approach relies on a circuit of plates whose motions can be inferred by fitting the crossings of magnetic anomalies and fracture zones on one side of a mid-ocean ridge that separates a pair of plates to coeval crossings on the other side of the ridge. For example, to estimate the motion between the Pacific and North American plates, researchers estimate the motion of

the African plate relative to the North American plate from the record of sea-floor spreading across the central Mid-Atlantic Ridge. In turn, the motion of the African plate relative to the Antarctic plate is estimated from the record of sea-floor spreading across the Southwest Indian Ridge, and the motion of the Pacific plate relative to the Antarctic plate is estimated from the record across the Pacific-Antarctic Rise (Fig. 1A). These motions are summed to estimate the motion of the Pacific relative to the North American plate (1). The motion of other oceanic plates relative to North America can be inferred from their motion relative to the Pacific plate and the

motion of the Pacific plate relative to North America. The motion of other continental plates can be incorporated from their motion relative to Antarctica, Africa, or North America.

The second approach is based on the assumption that the Pacific hotspots, such as the volcanic source of Hawaii, are fixed (that is, do not move) relative to the Atlantic hotspots, such as the volcanic source of Tristan da Cunha island (2–5). Hotspot tracks include basaltic volcanic chains, ridges, oceanic plateaux, and flood basalts thought to be created as a plate moves over a mantle plume (6–10). If the hotspots are fixed relative to one another and serve as a mantle reference frame (11), the history of motion of a plate relative to the deep mantle can be estimated from the locations and ages of volcanic edifices along two or more tracks. In this approach, the motion of the North American plate relative to the African plate is estimated as in the first approach. The age and location of hotspot tracks on the African plate are used

Fig. 1. (A) Cartoon showing the global plate-motion circuit linking the Pacific plate to the continental plates. Arrows show plate reconstruction links across which motion can be determined from the locations of magnetic reversals and fracture zones preserved in the ocean floor on both sides of a mid-ocean ridge. To reconstruct the position of the North American plate relative to the Pacific plate 49 million years ago (Ma), for example, the North American plate is rotated relative to the African plate, then the African and North American plates are rotated together relative to the Antarctic plate, and lastly the Antarctic, African, and North American plates are rotated as a unit relative to the Pacific plate. Direct reconstructions of the North American plate into the Pacific reference frame before ~3 Ma are impossible because this plate pair lacked an intervening mid-ocean ridge. The regions separating East from West Antarctica and the North from the South Pacific (ruled pattern) are zones where additional plate boundaries are suspected but are unmodeled in the global plate circuit. If motion occurs on one or more unmodeled plate boundaries, then the global plate-motion circuit will be systematically in error. (B) If hotspots under the North Pacific plate are fixed relative to those under the African plate, the hotspot circuit provides an alternative reconstruction path. The other continental plates can be added with use of the links shown in (A). If all the apparent motion between Pacific and Atlantic hotspots resulted from motion between East and West Antarctica, this circuit could be used to determine how much motion is required between East and West Antarctica. Plate abbreviations: AF, Africa; AN, Antarctica (W, west; E, east); AU, Australia; EU, Eurasia; GR, Greenland; IN, India; NA, North America; PA, Pacific; and SA, South America. HS, hotspots.



G. D. Acton is with the Department of Earth and Planetary Sciences, University of New Mexico, Albuquerque, NM 87131–1116, USA. R. G. Gordon is with the Laboratoire de Géodynamique Sous-Marine, B.P. 48, 06230 Villefranche sur Mer, France.

*Present address: Department of Geology and Geophysics, University of New England, Armidale, NSW 2351, Australia.

†Present address: Department of Geological Sciences, Northwestern University, Evanston, IL 60208, USA.

to estimate the motion of the African plate relative to the hotspots across which it has moved (12). Similarly, the age and location of hotspot tracks on the Pacific plate are used to estimate the motion of the Pacific plate relative to the hotspots. These motions are summed to estimate the motion of the Pacific plate relative to the North American plate. As above, other plates can be incorporated by summing their motion relative to the Pacific, (East) Antarctic, African, or North American plates (Fig. 1B).

If the hotspots beneath the African plate are fixed relative to those beneath the Pacific plate, if the plates are rigid, and if all the ancient plate boundaries have been recognized and incorporated, then the two sets of reconstructions should agree within their uncertainties. Earlier work has indicated that the two sets of reconstructions differ significantly (13). Molnar and Stock (13) concluded that the cause of the difference is motion between hotspots, with the Tristan da Cunha and other non-Pacific hotspots having moved relative to the Hawaiian hotspot at speeds of 10 to 20 mm/year over the past 70 My. These speeds are similar to the slowest speeds, about one-tenth as fast as the fastest speeds, at which adjacent plates move relative to one another.

If this interpretation (13) is correct, the resulting estimates of motion between hotspots would provide an estimate of the horizontal motion between mantle plumes and therefore provide information on horizontal velocities of convection within the part of the mantle through which plumes rise. Unfortunately, however, if the interpretation is correct, reconstructions found by assuming no motion between hotspots have large errors attributable to this motion and any reference frame for plate motion found by assuming no motion between hotspots has limited use. The hotspot frame of reference has been widely used by paleomagnetists to infer true polar wandering and by geodynamicists to make inferences about the driving forces of plate motion and

mantle convection. Thus, if the differences are indeed caused by motions between hotspots, a large body of inferences is invalid.

Analyses of paleomagnetic data have long suggested, however, that the hotspots provide a useful frame of reference for plate motion. Morgan (8), using the analyses of Andrews (14), constructed an apparent polar wander path for the hotspots in the Atlantic and Indian oceans. An apparent polar wander path is a time sequence of paleomagnetic poles relative to a stable reference frame, usually coinciding with a continent or plate; paleomagnetic poles are presumed to coincide with the past position of Earth's axis of rotation. Hence, paleomagnetic poles of similar age from different plates should coincide (within uncertainties) in location after the plates and poles are reconstructed at that age into a common reference frame. If the Pacific hotspots have been fixed relative to non-Pacific hotspots, then the apparent polar wander path from non-Pacific data predicts that the Hawaiian and other Pacific hotspots have moved southward relative to the paleomagnetic axis since ~65 million years before present (Ma) (8). The paleolatitude of Suiko seamount determined from paleomagnetic study of flows recovered by deep-sea drilling confirms this predicted southward motion (8, 15), as do other paleomagnetic data (16) and analyses of equatorial sediment facies (17).

Earlier paleomagnetic tests of the global plate-motion circuit furthermore have found that the reconstructions fail to bring Pacific paleomagnetic poles into consistency with non-Pacific paleomagnetic poles (18–20). The inconsistency of paleomagnetic data with the global plate circuit and the success of paleomagnetic predictions based on the hotspot circuit helped to persuade Engebretson *et al.* (5) to develop reconstructions based on the assumption of fixed hotspots rather than on the global plate-motion circuit.

A further reason to suspect the correctness of plate motions deduced from the

global plate-motion circuit comes from early Tertiary plate velocities relative to the deep mantle calculated with the assumption that the lithosphere, the strong outer layer of Earth comprising the plates, exerts no net torque on the asthenosphere (21), the weaker underlying layer. Early Tertiary plate velocities estimated from these no-net-torque calculations on the basis of the global plate-motion circuit have characteristics inconsistent with our understanding of the dynamics of plate motion (22). For example, an oceanic plate was estimated to have retreated from, rather than advanced toward, the deep-sea trench where its leading edge was being subducted; some continental plates unattached to subducting slabs were calculated to have moved rapidly. In contrast, early Tertiary plate velocities calculated with the assumption of fixed hotspots give a set of velocities with characteristics like present plate motions and are consistent with our understanding of plate dynamics (23–25).

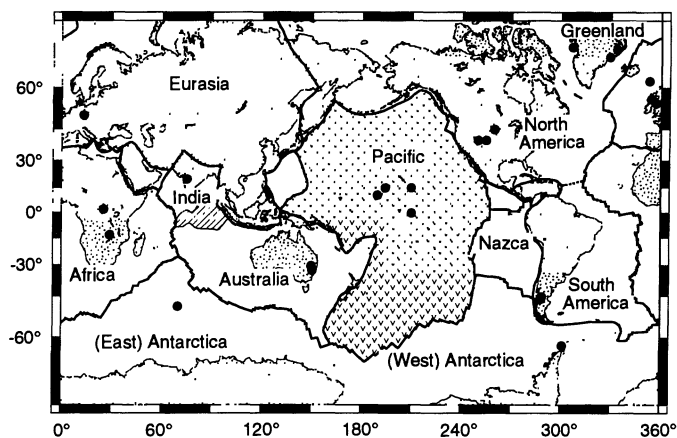
The most likely explanation for these inferred errors in the global plate-motion circuit has long seemed to be a missing plate boundary somewhere between East Antarctica and the North Pacific (3, 8, 19, 20, 25–27). A subsequently proposed candidate for this missing plate boundary is one that now lies within the Antarctic plate; its existence was inferred from a reinterpretation and quantitative analysis of the locations of magnetic anomaly crossings in the South Pacific east of New Zealand (28). The analysis of Molnar and Stock (13), in which they found motion of 10 to 20 mm/year between hotspots, is based on this revised global plate-motion circuit. If all boundaries have now been identified and appropriately incorporated, then Pacific plate paleomagnetic poles ought to be consistent with non-Pacific poles reconstructed through this revised global plate-motion circuit.

We used paleomagnetic poles to test the revised global plate circuit since ~70 Ma. For these tests, we compiled a set of 24 mean poles averaged from all available high-quality paleomagnetic data, which came from 78 studies on nine plates (Fig. 2) (29). The poles from the non-Pacific plates are reconstructed into a reference frame in which the Pacific plate is held fixed. Our tests differ from earlier tests not only in the incorporation of many new data but also in the incorporation of error budgets for each paleomagnetic pole that include estimates of plate-reconstruction errors, random paleomagnetic errors, and systematic paleomagnetic errors.

Paleomagnetic Test of the Reconstructions

Each of the 24 mean poles, which range in age from 20 to 73 Ma, is typically the average of several formation mean poles.

Fig. 2. Mean paleomagnetic data localities (solid circles) and present geometry of the major lithospheric plates. Between Greenland and North America, the location of a former spreading center is shown by a dashed line where spreading ceased ~40 Ma. The equatorial region near 80°E (ruled pattern) is the approximate location of the wide plate boundary zone between the Indian and Australian plates. Mercator's projection.



There are three mean poles from Africa, two from Antarctica, two from Australia, four from Eurasia, three from Greenland, one from India, three from North America, two from South America, and four from the Pacific plate. The basic data used to estimate the mean poles are from ~14,100 fully oriented paleomagnetic samples, 1600 paleomagnetic samples from azimuthally unoriented cores, seven seamount poles, two effective magnetization inclinations from submarine volcanic ridges, 11 identifications of equatorial sediment facies, and 182 estimates of the skewness of (30) and 2 estimates of the amplitudes of (31) magnetic anomalies that record ancient sea-floor spreading in the Pacific.

Plate reconstructions are specified by rotations of plates, which are idealized as rigid spherical caps. The parameters that describe these rotations are imperfectly known, and each reconstruction has an uncertainty associated with it. Hence, when a paleomagnetic pole is reconstructed from its indigenous frame of reference into that fixed to a foreign plate, its uncertainty is a combination of its uncertainty in its indigenous frame of reference and further uncertainty caused by the uncertainty in the reconstruction (32, 33). The final uncertainty in the position of a reconstructed paleomagnetic pole is a combination of the original uncertainty in the paleomagnetic pole and the uncertainty that accumulates as the paleomagnetic pole is reconstructed through multiple links of the plate circuit (34).

The means of the non-Pacific poles reconstructed into the Pacific reference frame show a surprising pattern: The poles for 27, 46, and 56 Ma sit atop one another in standstill with the reconstructed mean pole for 66 Ma located ~7° away (Fig. 3, stars) (Table 1). The observed Pacific plate poles are offset from these with a similar but less distinctive pattern, with the poles for 26, 39, and 58 Ma lying near one another but offset by ~7° from the pole for 65 Ma (Fig. 3, squares). Despite the large errors of some poles, Pacific plate poles differ significantly from coeval reconstructed mean non-Pacific poles. The difference between each Pacific pole and the corresponding mean, coeval, reconstructed, non-Pacific pole is significant at the 95% confidence level. These differences would be even larger and more significant if we had included the West Antarctic pole (Fig. 3, triangle) or had omitted the North American poles, which differ significantly from the non-North American poles (Table 1) (29, 35). For normal-polarity results, the reconstructed non-Pacific poles tend to predict lower (that is, more negative) inclinations (corresponding to less northward motion of the Pacific plate) and more westerly declinations for Pacific plate sites than is predicted

by the Pacific poles (Fig. 3 and 4).

The angular distance between each Pacific plate pole and the corresponding coeval, mean, reconstructed non-Pacific pole

is $9.6^\circ \pm 9.5^\circ$, $9.4^\circ \pm 4.1^\circ$, $9.6^\circ \pm 5.0^\circ$, and $9.7^\circ \pm 3.5^\circ$, respectively, for the poles at 26, 39, 58, and 65 Ma (36). Estimates of angular distance, like all estimates of distance, are

Fig. 3. Observed and predicted paleomagnetic poles for the Pacific plate assuming a purely dipolar paleomagnetic field. Solid squares and surrounding open ellipses are the paleomagnetic poles and their 95% confidence limits from the Pacific plate. Solid stars and surrounding diagonally striped ellipses with dashed outlines are the paleomagnetic poles and their 95% confidence limits of the averages of many poles reconstructed from the rest of Earth into a reference frame in which the Pacific plate is held fixed. The confidence limits of the mean reconstructed poles, which are determined from nonoverlapping data sets, incorporate both paleomagnetic uncertainties and plate reconstruction uncertainties (70). The open triangle and surrounding dotted ellipse shows the 51-Ma pole for West Antarctica reconstructed into the Pacific plate reference frame. The numerals following PA (Pacific plate), AN (Antarctica), or RG (the rest of the globe) give the age of each pole in millions of years. The significant difference between Pacific poles and mean reconstructed non-Pacific poles indicates a systematic error of unknown cause in the global plate reconstruction circuit through the South Pacific and Antarctica. Stereographic projection.

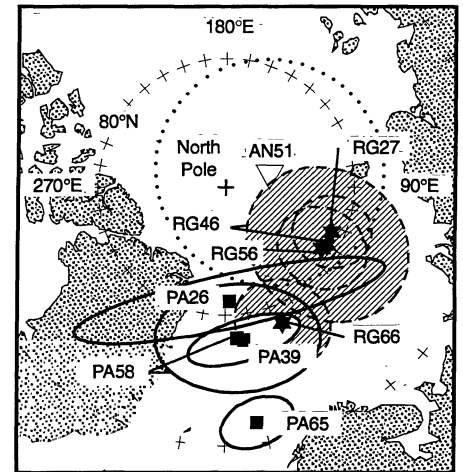


Table 1. Paleomagnetic poles. Lat., latitude; Long., longitude.

Name*	Position		χ_v^\dagger	ν^\ddagger	Standard error ellipse§			Reference or poles used
	Lat. (°N)	Long. (°E)			Major	Minor	Az	
<i>Pacific poles</i>								
PA26	81.1	2.4	0.41	14	7.1°	1.2°	80.0°	Acton and Gordon (29)
PA39	78.0	7.1	0.60	6	2.6°	0.9°	80.0°	Acton and Gordon (29)
PA58	78.2	4.8	1.00	129	4.8°	3.7°	93.0°	Petronotis <i>et al.</i> (62)
PA65	71.6	7.9	1.02	57	1.7°	1.0°	75.0°	Acton and Gordon (74)
<i>Reconstructed mean poles</i>								
RG27	81.0	67.4	1.19	6	1.8°	1.6°	171.0°	AF26 AN27 EU25 NA30
RG39	80.8	59.7	1.52	8	2.1°	1.9°	8.5°	AF40 AN27 NA30 NA49 SA49
RG42	81.0	60.6	1.93	6	2.4°	2.2°	9.4°	NA30 AF40 NA49 SA49
RG44	79.1	80.5	0.59	2	3.3°	2.5°	14.5°	AF40 SA49
RG46	80.9	60.7	2.89	4	3.8°	3.3°	7.2°	AF40 NA49 SA49
RG50	82.1	60.9	2.47	6	3.2°	2.8°	1.4°	AF40 AN51 NA49 SA49
RG53	81.4	59.8	1.19	18	1.7°	1.5°	4.2°	AF40 AU53 EU53 EU57 EU60 GR52 GR55 GR60 NA49 SA49
RG55	82.0	57.7	1.05	14	2.0°	1.7°	170.8°	AN51 AU53 EU53 EU57 EU60 GR52 GR55 GR60
RG56	81.1	57.8	0.96	12	2.1°	1.8°	177.7°	AU53 EU53 EU57 EU60 GR52 GR55 GR60
RG58	81.4	62.3	1.00	6	2.6°	2.4°	171.2°	EU57 EU60 GR55 GR60
RG63	80.2	29.1	2.05	8	2.9°	2.4°	157.5°	AF65 IN65 EU60 GR60 NA63
RG64	80.1	28.2	1.69	10	2.4°	2.1°	156.6°	AF65 IN65 EU60 GR60 NA63 SA73
RG66	78.5	23.0	0.91	6	2.2°	1.9°	136.8°	AF65 IN65 NA63 SA73

*The Pacific poles (PA) incorporate data only from the Pacific plate. The reconstructed mean poles (RG) incorporate data from other plates that have been reconstructed into the frame of reference in which the Pacific plate is held fixed; they incorporate no Pacific plate data. The numbers give the mean age of the pole (in millions of years). The poles averaged to give the mean poles are listed in the right column (29). For example, pole RG66 has a mean age of 66 Ma and is an average of the reconstructed poles AF65, IN65, NA63, and SA73 (plate codes as in Fig. 1). †The value of the reduced chi-square statistic; if χ_v was greater than 1.0 for a mean pole, the uncertainty ellipse was rescaled for further calculations by multiplying the ellipse axes by the square root of reduced chi square. ‡Number of degrees of freedom. §Major, Minor, and Az give the length of the major and minor semiaxis and the azimuth of the major semiaxis (measured clockwise of north) for the two-dimensional standard error ellipse. The 95% confidence ellipse was estimated from the two dimensional standard error ellipse by multiplying the major and minor axes by the square root of the appropriate value of $F_{2, \nu}^{0.05}$, which can be obtained from standard tables for the F distribution for the 5% level of significance with two versus ν degrees of freedom. For example, the 95% confidence ellipse for pole RG66 has a 5.0° ($=2.2 \times \sqrt{5.14}$, where $5.14 = F_{2, 6}^{0.05}$) major axis oriented 136.8° clockwise of north and a 4.3° ($=1.9 \times \sqrt{5.14}$) minor axis.

biased; they tend to be larger than the true angular distance (37). We estimated the unbiased angular distances and their 95% confidence limits using Monte Carlo simulations. The unbiased angular distances are $9.1^{\circ} \pm 9.3^{\circ}$, $9.5^{\circ} \pm 4.1^{\circ}$, $9.3^{\circ} \pm 4.9^{\circ}$, and $9.6^{\circ} \pm 3.5^{\circ}$, respectively, for the poles at 26, 39, 58, and 65 Ma (38). The relative uncertainties for the unbiased estimates are slightly larger than those for the original biased estimates (39). All angular distances between paleomagnetic poles that we give below are corrected for the bias, and their confidence limits have been enlarged accordingly.

Thus far, we have assumed that the paleomagnetic field from 73 to 20 Ma was that of a geocentric axial dipole. An important alternative that must be considered is

that the time-averaged paleomagnetic field was imperfectly dipolar. Several studies of Cenozoic paleomagnetic data have suggested that the field may have also contained a small persistent geocentric axial quadrupole (GAQ) component of the same sign as the dipole component (40). Repeating the same tests as above with a paleomagnetic field with a 5% GAQ component of the same sign as the dipole component (that is, $g_2^0/g_1^0 = 0.05$) decreases the inconsistency but fails to eliminate it. The Pacific poles for 39, 58, and 65 Ma (but not the pole for 26 Ma) differ at the 95% confidence level from their mean coeval, reconstructed counterparts (41).

If instead a 10% GAQ component is assumed, the difference between Pacific and

non-Pacific poles is further reduced. Although the poles for 26 and 39 Ma differ insignificantly from their mean reconstructed counterparts, the poles for 58 and 65 Ma differ at the 95% confidence level from their counterparts (42). A persistent axial quadrupole component this large is far-fetched, however. A simple model of Earth's paleomagnetic field indicates that g_2^0/g_1^0 is only 0.04 ± 0.04 (29). If all poles are calculated assuming the best available estimate of the axial quadrupole term, that is, for a paleomagnetic field with $g_2^0/g_1^0 = 0.04$, the mean discrepancy is reduced by only ~ 230 km ($\sim 2.0^{\circ}$) relative to a purely dipolar field.

Comparison of the Paleomagnetic and Hotspot Discrepancies

As mentioned in the introduction, some evidence has previously been interpreted as indicating that Pacific hotspots move rapidly relative to Atlantic and Indian Ocean hotspots. For example, the locations and ages of volcanoes along the Hawaiian-Emperor chain differ from a track predicted from (i) a combination of Africa-Antarctica and Antarctica-Pacific reconstructions and (ii) the motion inferred for the African plate over the Tristan da Cunha and other hotspots (Fig. 5) (13, 43). Similarly, locations and ages of volcanoes produced by hotspots now at or near Iceland, Tristan da Cunha, Réunion, St. Paul's Island, and Kerguelen Island differ significantly from tracks predicted from (i) a combination of Africa-Antarctica and Antarctica-Pacific reconstructions and (ii) the motion inferred for the Pacific plate over the Hawaiian and other Pacific hotspots (13). Molnar and Stock (13) interpreted these differences as indicating that the Hawaiian hotspot has moved relative to Atlantic and Indian Ocean hotspots at 10 to 20 mm/year. We propose an alternative explanation: systematic errors in the global plate-motion circuit (Fig. 1).

If a systematic error exists in the global plate-motion circuit, one would expect the paleomagnetic discrepancy to be identical in direction and size to the hotspot discrepancy, which is a prediction that can be tested. Molnar and Stock (13) illustrated the hotspot discrepancy by comparing the observed and predicted track of the Hawaiian hotspot (as described above). The discrepancy has two components, a northward and a westward component, but three parameters are needed to specify the reconstruction of a plate relative to the hotspots.

In the case of a reconstruction of the Pacific plate relative to Pacific hotspots, the extra component corresponds to a rotation about a geocentric axis through the Hawaiian hotspot and is indeterminate from the Hawaiian hotspot track alone. Additional

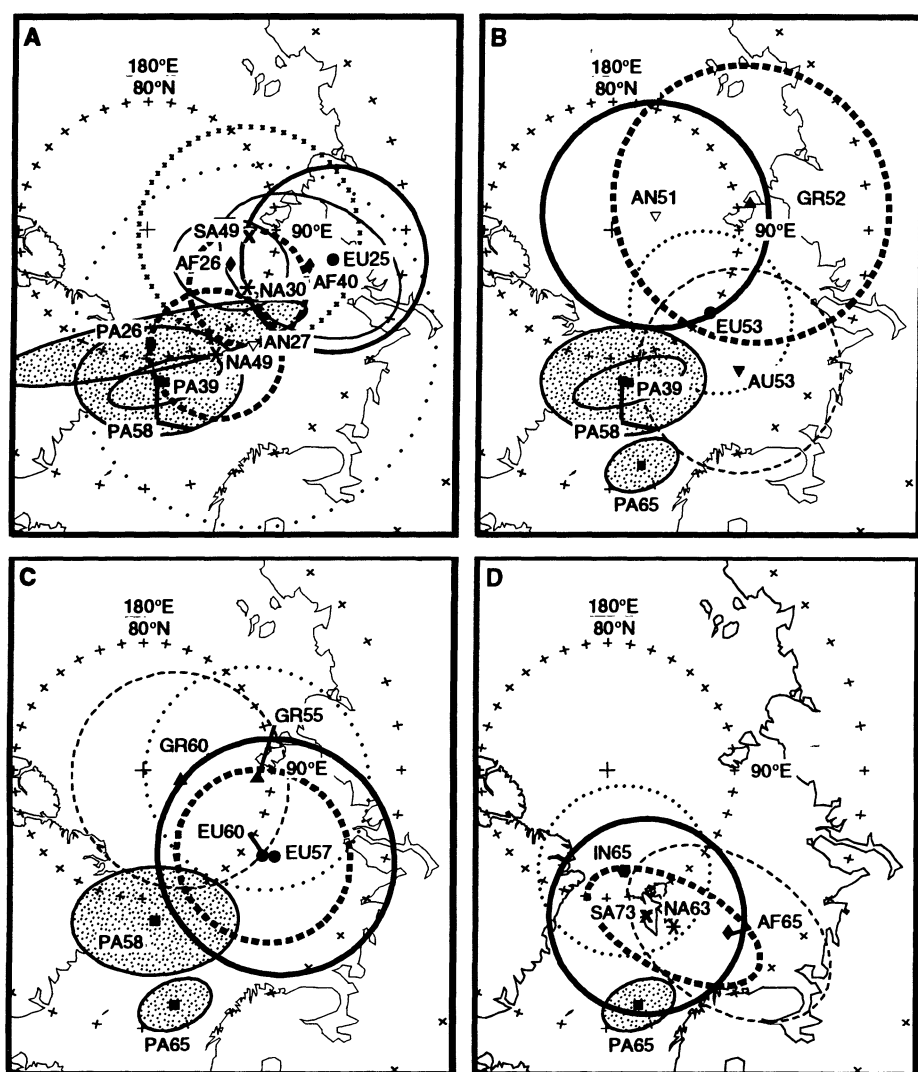


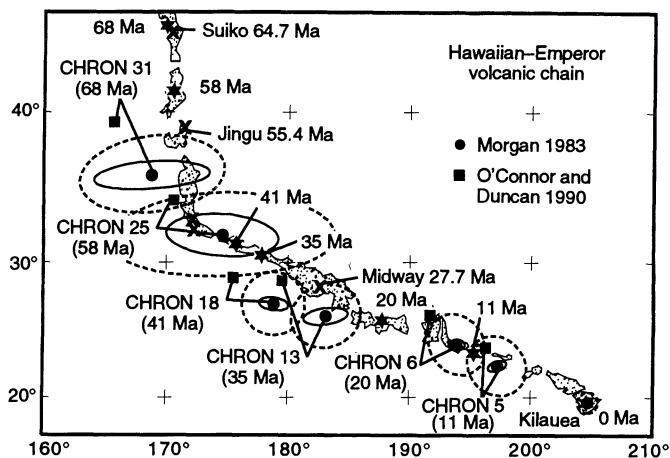
Fig. 4. Comparison of observed Pacific plate paleomagnetic poles with individual reconstructed mean poles assuming a purely dipolar paleomagnetic field. Age of comparison increases from (A) to (D). Squares and shaded ellipses are the paleomagnetic poles and their 95% confidence limits from the Pacific plate. Other symbols and open ellipses are individual reconstructed paleomagnetic poles and their 95% confidence limits, which include reconstruction uncertainties. The poles have a two-letter plate abbreviation (as in Fig. 1) followed by two numbers that give the age (in millions of years). All poles are in a reference frame in which the Pacific plate is held fixed. Nearly all the reconstructed poles differ significantly from the Pacific pole nearest in age (35). Stereographic projection.

Pacific hotspot tracks or further assumptions are needed to estimate the extra component. On the other hand, the Pacific paleomagnetic discrepancy also has two components, corresponding to the paleomagnetic inclination and declination at an arbitrarily chosen reference site, which we take to coincide with the point along the Hawaiian-Emperor chain having the same age as the paleomagnetic pole. This reference site was presumably over the hotspot at the time corresponding to the age of the paleomagnetic pole. The inclination can be transformed by simple calculation into the northward-motion component, and the declination gives the rotation about an axis through the Hawaiian hotspot. The paleo-longitude of the site is indeterminate from only a paleomagnetic pole. Thus, the two discrepancies have in common only the northward component of motion.

The northward motion of the Pacific plate relative to the hotspots is expected to differ from its northward motion relative to the paleomagnetic axis because the hotspots have moved relative to the paleomagnetic axis (44). What we therefore compare for each marker is the discrepancy between the northward motion indicated by Pacific plate data and that predicted from non-Pacific data and the global plate circuit. The northward motion of the Pacific plate relative to the hotspots recorded by the Hawaiian-Emperor seamount chain is the difference between the present latitude of an extinct volcano along the chain and the present latitude of the hotspot (Fig. 6). The northward motion predicted from the global plate circuit assuming fixed hotspots is the difference between the latitude (45) of the reconstructed position of the Hawaiian hotspot at some time in the past and the present latitude of the hotspot. The discrepancy between the northward motion inferred from the Hawaiian-Emperor chain (that is, the observed northward motion) and the predicted northward motion is $1.7^\circ \pm 2.2^\circ$ (190 ± 240 km) at 20 Ma, $4.2^\circ \pm 2.2^\circ$ (470 ± 240 km) at 35 Ma, $4.1^\circ \pm 2.2^\circ$ (460 ± 240 km) at 41 Ma, $9.5^\circ \pm 2.5^\circ$ (1060 ± 280 km) at 58 Ma, and $8.8^\circ \pm 2.3^\circ$ (980 ± 260 km) at 68 Ma (Fig. 6) (46).

The discrepancy between the northward motion inferred from Pacific plate paleomagnetic poles (that is, the observed northward motion) and that predicted from mean reconstructed non-Pacific paleomagnetic poles for a dipole field is $4.1^\circ \pm 3.1^\circ$ (460 ± 340 km) at 26 Ma, $7.5^\circ \pm 3.3^\circ$ (830 ± 370 km) at 39 Ma, $7.7^\circ \pm 4.1^\circ$ (860 ± 460 km) at 58 Ma, and $9.6^\circ \pm 3.5^\circ$ (1070 ± 480 km) at 65 Ma (Fig. 7). The discrepancies between the predicted and observed paleomagnetically determined northward motions differ insignificantly in size and sense from the discrepancies found from the hot-

Fig. 5. Observed and predicted track of the Hawaiian hotspot. Key observed ages (x's) and interpolated and extrapolated ages (stars) are shown along the Hawaiian-Emperor volcanic chain, which presumably formed as the Pacific plate moved over the Hawaiian plume. The two unlabeled x's at the elbow of the Hawaiian-Emperor chain show the position of the Daikakuji Seamount (southern x) with an age of 42.4 ± 2.3 Ma and the Yuryaku Seamount (northern x) with an age of 43.4 ± 1.6 Ma (71). Solid dots and surrounding solid ellipses show the predicted locations and 95% confidence limits of the Hawaiian hotspot track that we obtained by using the Africa hotspot reconstructions of Morgan (66) and by ignoring the uncertainty in the Africa hotspot reconstructions. These positions and uncertainties are similar to those shown in figure 1 of (13). The dashed ellipses show the 95% confidence for the predicted locations when we incorporate nominal uncorrelated ± 100 -km ($\pm 1\sigma$) uncertainties in the Africa hotspot reconstructions at the location of the Tristan hotspot in directions both parallel and perpendicular to the Walvis Ridge. The age for each prediction is given in parentheses beneath the chron number of the corresponding reconstruction. Solid squares show the locations of the Hawaiian hotspot track predicted with the Africa hotspot reconstructions of O'Connor and Duncan (69). Uncertainties that we calculated for these locations (not shown) are nearly identical to the corresponding, coeval dashed ellipses shown for the dots. Comparison of predicted with observed tracks show large formally significant differences, which have previously been interpreted as indicating large displacements of the Hawaiian hotspot relative to Atlantic hotspots. The difference may instead reflect a large systematic error in the plate reconstructions. To facilitate comparison, reconstructed points and their uncertainties are presented in a manner similar to figure 1 of (13).



spots. Thus, the results are consistent with a systematic error in the global plate circuit having contributed to both the paleomagnetic and hotspot discrepancies, but the uncertainties are so large that one could only place large upper limits on how much of the misfit is contributed by other causes, especially motion between hotspots and systematic errors in the hotspot reconstructions (47).

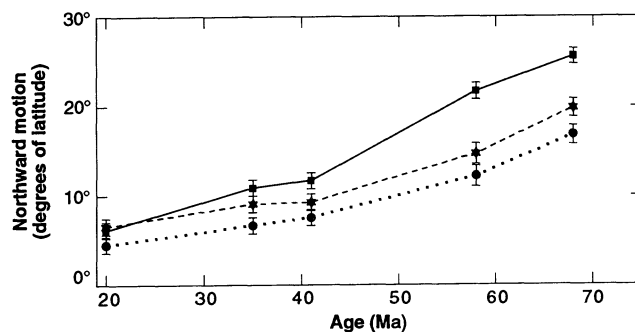
The Cause of the Discrepancies

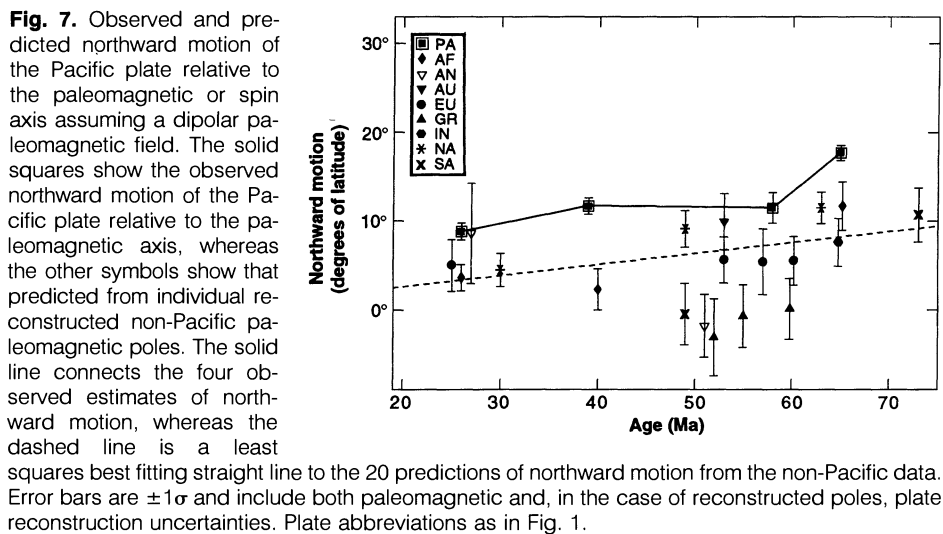
Possible systematic errors in the plate reconstructions include (i) underestimation of the size of all plate reconstruction errors,

(ii) a systematic error in the reconstruction of East Antarctica relative to the North Pacific (all non-Pacific data were rotated through this common link) or in the reconstruction of the African plate relative to East Antarctica (all but four non-Pacific poles were rotated through this link), (iii) plate nonrigidity or many zones across which minor deformation has occurred, and (iv) ignorance of a major plate boundary active since 80 Ma.

The first explanation seems unlikely because it would require that magnetic anomalies or fracture zones had been systematically misidentified or wrongly correlated across a spreading center by enough to add

Fig. 6. Observed and predicted northward motion of the Pacific plate relative to the hotspots. Squares show the observed northward motion of the Pacific plate relative to the Hawaiian hotspot. Circles and stars show the northward motion of the Pacific plate relative to the Hawaiian hotspot predicted by global plate reconstructions and by assuming that the Hawaiian hotspot is fixed relative to Atlantic hotspots. The circles are determined from the Africa-hotspot rotations of Morgan (66), whereas the stars are determined from those of O'Connor and Duncan (69). Error bars for the solid circles show uncertainties of $\pm 1\sigma$. Uncertainties in ages, which may be substantial, are not shown.





up to a systematic reconstruction error of about 500 to 1000 km and that this error had been repeated for reconstructions of different ages. In the particular case of the Indian Ocean, the credibility of the error budget has been implicitly tested by Royer and Chang (48); their results suggest that the errors tend not to be underestimated but to be slightly overestimated.

The second explanation is unlikely in the Indian Ocean because there are enough marine magnetic anomaly and fracture zone

crossings between Africa and Antarctica to make large systematic errors unlikely. Recent data from the Antarctic side of the Pacific-Antarctic Rise also indicate that there are no large systematic errors from this source (49).

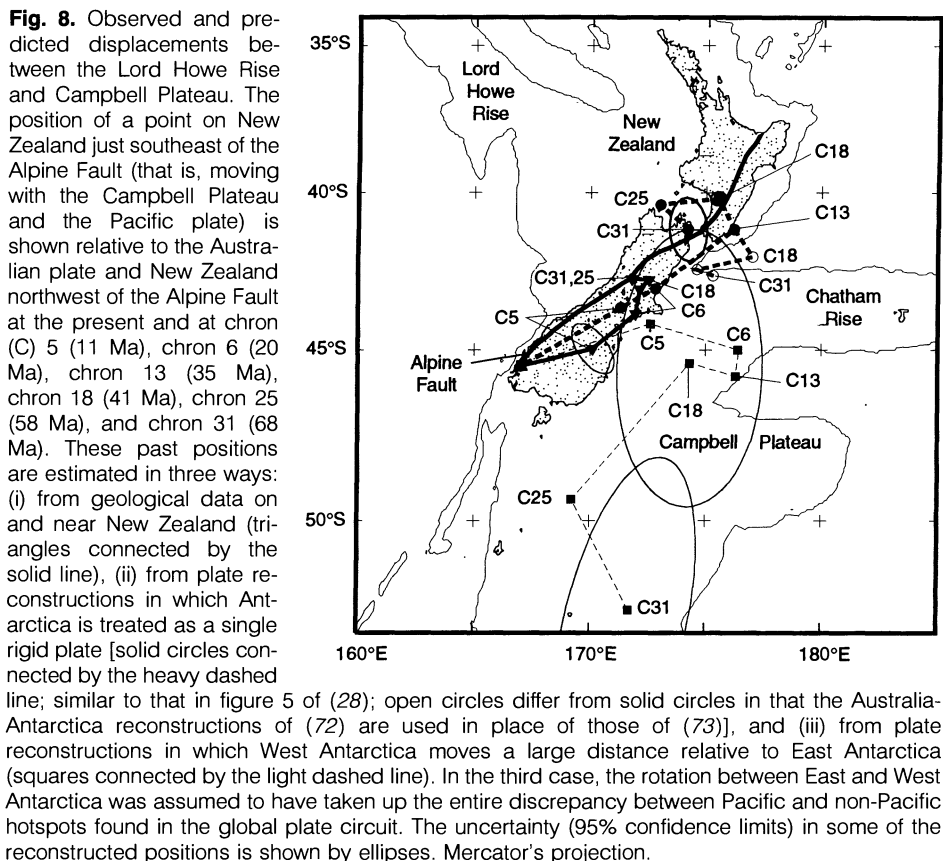
The third explanation probably requires larger than acceptable intraplate strains in the southern hemisphere. The average location where Pacific paleomagnetic data were obtained (that is, the northern Pacific) and the average location where non-

Pacific data were obtained are separated by $\sim 20,000$ km ($\sim 180^\circ$). The Pacific discrepancy at 60 Ma is $\sim 1000 \pm 600$ km, which gives an average strain of $\sim 5 \pm 3\%$, which is huge by any standard. The sense of the misfit indicates that the strain would have been mainly extensional along the plate-motion circuit. If this deformation occurred between 60 and 20 Ma, then the summed rate of displacement is $\sim 25 \pm 15$ mm/year. Alternatively, if it occurred mainly between 60 and 40 Ma, then the displacement rate would have been $\sim 50 \pm 30$ mm/year.

These summed deformation rates, if entirely taken up by distributed deformation, seem implausibly large. Systematic misfits to plate motion data by recent global models of current plate motion do not exceed ~ 3 mm/year (50). Plate motion data in the Indian Ocean place upper 95% confidence limits on deformation of a circuit traversed near and about the Rodriguez (Indian Ocean) triple junction of ~ 4 to 7 mm/year (51). North American sites with the best geodetic data from very-long-baseline interferometry cannot be moving faster than 3 or 4 mm/year relative to the rest of the North American plate and may be moving much more slowly (52). Thus, current rates of intraplate deformation are probably no more than 3 or 4 mm/year and possibly much less. The ancient plate-motion circuit through the South Pacific and Antarctica crosses too few plates to add up to 25 to 50 mm/year of deformation. Intraplate deformation can explain the discrepancy only if the discrepancy is no larger than about 10 mm/year, which is the lower confidence limit obtained assuming the longest conceivable duration of deformation (that is, 40 My).

The fourth explanation can be tested either paleomagnetically or by examining whether the plate motion implied across the hypothesized boundaries and other plate boundaries is consistent with available or obtainable geological and geophysical data. We consider two specific possibilities: (i) motion between East and West Antarctica and (ii) motion between distinct North and South Pacific plates.

Motion between East and West Antarctica. Geological and geophysical evidence suggests that West Antarctica has moved relative to East Antarctica since ~ 65 Ma. The existence of the Transantarctic Mountains, which form a 3000-km-long boundary separating East from West Antarctica, is the most conspicuous evidence. The rocks that form these mountains have risen ~ 5 km since 50 Ma at an average rate of ~ 100 m/My (53). The uplift is thought to be a flexural or thermal response to extension (54, 55). Other evidence for extension between East and West Antarctica since ~ 70

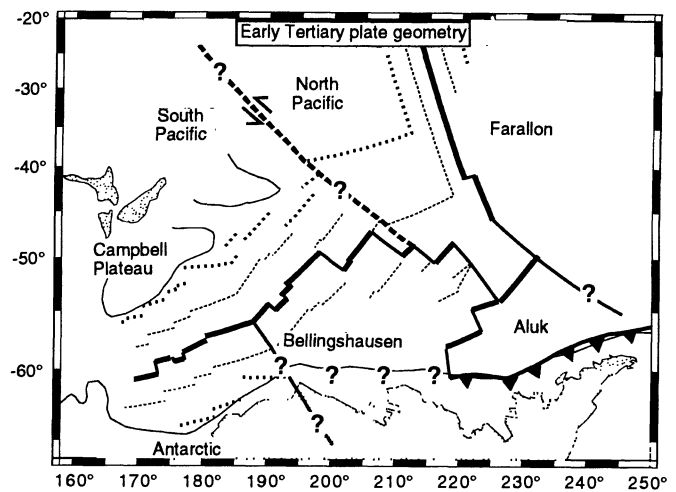


Ma includes the presence of block faulted basins and high heat flow (70 mW/m^2) (56) in the Ross Sea region, the presence of Miocene-age volcanic rocks along the western margin of East Antarctica, and an abrupt change in crustal thickness from West Antarctica (25 to 30 km thick) to East Antarctica (40 to 45 km thick) (54, 57).

If the hotspots are fixed, the motion between East and West Antarctica required to explain the entire discrepancy can be estimated. The motion of West Antarctica relative to the hotspots is estimated with use of the West Antarctic–Pacific hotspot circuit, and the motion of East Antarctica relative to the hotspots is estimated with use of the East Antarctic–Africa hotspot circuit (Fig. 1B). The inferred stage poles of rotation of West Antarctica relative to East Antarctica are typically near the West Antarctic coast ($\sim 65^\circ\text{S}$, 135°E) for reconstructions younger than 32 Ma, but lie relatively far from Antarctica and at low latitudes (between $\sim 1^\circ\text{S}$ and 35°S , near 100°E) for reconstructions at 50 to 70 Ma when described in the East Antarctic reference frame. For an assumed paleo–plate boundary mainly following the seaward edge of the Transantarctic Mountains, the analysis indicates ~ 800 km of left-lateral strike-slip between East and West Antarctica between 70 and 40 Ma, and ~ 500 km of extension with some left-lateral slip since 40 Ma. The sense, magnitude, and timing of this inferred motion does not seem inconsistent with the known record of tectonics of Antarctica.

Data from New Zealand, however, impose smaller limits on motion between East and West Antarctica. If we incorporate motion between East and West Antarctica calculated assuming fixed hotspots (as described above) and if the past plate boundary geometry between Lord Howe Rise and the Campbell Plateau was similar in location and strike to the current Alpine Fault, we calculate the following predicted motion across the Alpine fault: ~ 300 km of contraction from geomagnetic-reversal chron 31 (68 Ma) to chron 25 (58 Ma), ~ 500 km of left-lateral slip and some contraction from chron 25 to chron 18 (41 Ma), little or no motion from chron 18 to chron 6 (20 Ma), about 300 km of contraction and right-lateral slip from chron 6 to chron 5 (11 Ma), and about 350 km of right-lateral slip and 100 km of contraction since chron 5 (Fig. 8). The geologic data (58, 59) indicate a very different history with little or no motion before the Middle Eocene (~ 50 Ma), ~ 100 km of extension from the Middle Eocene to the Early Miocene (~ 23 Ma), and ~ 480 km of right-lateral slip and ~ 100 km of contraction since 23 Ma (Fig. 8). Thus, reconstructions that assume that hotspots are fixed and that the entire discrepancy is caused by motion between East

Fig. 9. Early Tertiary plate geometry in the south Pacific assuming a single Pacific plate since chron 25 (58 Ma). Bold lines are mid-ocean ridges; medium-bold lines are transform faults or speculative plate boundaries. Thick dotted lines are chron 34 (83-Ma) magnetic lineations, and thin dashed lines are chron 31 (68-Ma) magnetic lineations [lineation location from (60)]. Barbed line indicates trench where the Aluk plate is assumed to have subducted beneath the Antarctic peninsula. Plate geometry after (28) and (60). A possible location for the “suspect” plate boundary between North and South Pacific plates is shown by the thick dashed line. Mercator’s projection.



and West Antarctica are inconsistent with the observations.

On the other hand, recently determined plate reconstructions (28, 60), in which Antarctica is assumed to be a single rigid plate, are only modestly inconsistent with the geological constraints (Fig. 8), although an even better fit is obtained with 200 to 300 km of extension between East and West Antarctica during the Oligocene or Miocene (28, 59). Such extension would reduce the Pacific paleomagnetic and hotspot discrepancies. However, because the northward component of the paleomagnetic discrepancy is substantial and because the fixed hotspot reconstructions indicate equatorial stage poles of rotation between East and West Antarctica during the early Tertiary, modest extension between East and West Antarctica seems insufficient to explain the full discrepancy.

Motion between the North and South Pacific. Another seemingly unlikely explanation is that there were separate North Pacific and South Pacific plates for a long interval since 80 Ma (19, 20). Before ~ 80 Ma, the Campbell Plateau (the submerged continental plateau that is the southeast continuation of New Zealand) surely lay on a plate separate from the North Pacific. Many workers have assumed that the Campbell Plateau and adjacent sea floor fused with the North Pacific at ~ 80 Ma, when spreading began between the Campbell Plateau and Marie Byrd Land (West Antarctica). Available data neither demonstrate nor refute this conjectured age of fusion. If a boundary continued to exist between the North Pacific and the Campbell Plateau after 80 Ma, available evidence can, however, put broad limits on its location.

Magnetic anomaly and fracture zone crossings on the present Pacific plate south

of the Eltanin fracture zone system seem well explained by spreading between the Pacific and Antarctic plates and by spreading between the Pacific and Bellingshausen plates (26, 28, 60). Thus, any intersection of a boundary between possibly separate North and South Pacific plates with the Pacific–Antarctic Rise or East Pacific Rise probably lies north of this region, that is, at the Eltanin fracture zone system or farther north.

Magnetic anomaly and fracture zone crossings on the present Pacific plate north of the equator seem well explained by spreading between the Pacific plate and the Kula plate and by spreading between the Pacific plate and the Farallon plate and its descendants (61). Crossings a considerable distance south of the equator also seem explainable by spreading between the Pacific and Farallon plates. Past analyses of Pacific plate magnetic anomalies and fracture zones indicated that they are consistent with there having been a single Pacific and a single Farallon plate between ~ 50 and ~ 70 Ma as far south as 43°S (a little south of the Agassiz fracture zone) (61), but data from the South Pacific were sparse. Recent analysis of many more anomaly crossings shows that the data are now inconsistent with the joint hypotheses of a single rigid Pacific plate and a single rigid Farallon plate if spreading along the ancient East Pacific Rise was symmetrical (62). Although we think it unlikely that the Pacific was divided north of 43°S since 80 Ma, the data cannot exclude this possibility (63).

A more likely possibility for the location of the intersection of a North Pacific–South Pacific boundary with the East Pacific Rise or Pacific–Antarctic Rise is a region that begins at the Eltanin fracture zone system and extends north and northeast to 43°S . That

Late Cretaceous and early Tertiary spreading rates north of the Eltanin fracture zone system were much faster than rates just south of it shows that the plate pair that diverged along the Pacific-Antarctic Rise south of the Eltanin fracture zone differed from the plate pair that diverged along the East Pacific Rise north of it (64). The spacing of the magnetic anomalies above the ~45- to 80-My-old sea floor in this region is much wider than expected for either Pacific-Farallon spreading, as observed to the north, or for Pacific-Bellingshausen spreading, as observed to the south. Thus, yet another plate pair must have been separated along this segment of the East Pacific Rise.

Cande *et al.* (64) proposed that the spreading occurred between a single united Pacific plate northwest of the ancient East Pacific Rise and the Aluk plate southeast of the East Pacific Rise (Fig. 9) (65). They compared the Pacific-Aluk spreading rate north of the Eltanin fracture zone to the sum of Pacific-Bellingshausen and Bellingshausen-Aluk spreading south of the Eltanin fracture zone system. These rates are similar, consistent with their assumption of a single rigid Pacific plate northwest of the East Pacific and Pacific-Antarctic rises. Despite this consistency, their analysis neither demonstrates the absence of, nor places bounds on, motion between distinct North Pacific and South Pacific plates divided near the Eltanin fracture zone. The data constraining this zone are much sparser than the data available for estimating Pacific-Farallon or Pacific-Bellingshausen motion. Unlike the situation for these other two regions, no finite rotations, much less confidence limits, have been estimated for Pacific-Aluk spreading.

Until such estimates are available, the only observations available for testing the hypothesis that the South Pacific has moved independently from the North Pacific are paleomagnetic poles. Gordon and Cox (19) found significant differences between the paleomagnetic pole from the Chatham Island basalts (east of New Zealand) and a North Pacific pole they believed to be of the same age. Later revisions to the geomagnetic reversal time scale suggest, however, that their North Pacific pole is older than they assumed, so their test is inconclusive. Another test is provided by the 51-Ma pole from West Antarctica. When we reconstruct it into the Pacific plate reference frame, it indicates significantly less northward motion than do either of the poles from the Pacific plate for 39 or 58 Ma (Fig. 5). This difference suggests that the northern Pacific plate has moved substantially relative to the southern Pacific plate since 80 Ma, but is by no means convincing by itself. More paleomagnetic data are needed from New Zealand and from southern Pacific sea floor before this

comparison can give convincing results.

We speculate that the North Pacific and South Pacific plates remained distinct for some interval since ~80 Ma, possibly fusing as late as the time of the major change of motion of the North Pacific plate associated with the ~43-My-old elbow in the Hawaiian-Emperor chain. Motion between the North and South Pacific may have combined with motion between East and West Antarctica to produce all of the paleomagnetic discrepancy and all or part of the hotspot discrepancy.

Future Research Directions

We have shown that the global plate-motion circuit through Antarctica and the South Pacific fails a paleomagnetic test even after incorporation of plate reconstruction errors, systematic errors in the paleomagnetic data, recent revisions to the plate reconstructions, and a small persistent quadrupole component of the paleomagnetic field. The cause of this failure is unclear. More paleomagnetic poles from the South Pacific are needed to investigate whether they differ significantly from those of the North Pacific, where further paleomagnetic data would also be useful. Rotation parameters and confidence limits for both North Pacific-Aluk and Aluk-Bellingshausen plate motion are needed.

The existence of the discrepancies suggests that early Tertiary reconstructions using the global plate-motion circuit through Antarctica are systematically in error by about 810 ± 350 km and that these systematic errors have not been incorporated into previous estimates of the uncertainties of past plate positions inferred from the global plate-motion circuit. A large part of the difference between plate motions inferred from the global plate-motion circuit and those inferred from the fixed hotspot circuit may be attributable to this systematic error. This will remain a speculation, however, until more reliable confidence limits are available for plate motions inferred from the assumption of fixed hotspots. It follows that earlier estimates of motion between hotspots are also systematically in error, but our results do not place new useful bounds on the motion between hotspots. Instead, they indicate that these motions are known less well and may be smaller than previously believed. Further work, especially on estimating uncertainties of plate reconstructions relative to hotspots, is needed to place reliable bounds on the motion.

REFERENCES AND NOTES

1. T. Atwater and P. Molnar, in *Proceedings of the Conference on Tectonic Problems of the San Andreas Fault System*, R. L. Kovach and A. Nur, Eds. (Stanford University Publications in Geological Sciences, Stanford, CA, 1973), vol. 13, pp. 136-148.
2. P. J. Coney, *Am. J. Sci.* **272**, 603 (1972).
3. R. A. Duncan, *Tectonophysics* **74**, 29 (1981).
4. R. L. Carlson, *ibid.* **99**, 149 (1983).
5. D. C. Engebretson, A. Cox, R. G. Gordon, *Geol. Soc. Am. Spec. Pap.* **206** (1985).
6. J. T. Wilson, *Nature* **207**, 343 (1965).
7. W. J. Morgan, *ibid.* **230**, 42 (1971).
8. _____, in *Oceanic Lithosphere*, vol. 7 of *The Sea*, C. Emiliani, Ed. (Wiley-Interscience, New York, 1981), pp. 443-487.
9. L. J. Henderson and R. G. Gordon, *Eos* **62**, 1028 (abstr.) (1981).
10. R. A. Duncan and M. A. Richards, *Rev. Geophys.* **29**, 31 (1991).
11. W. J. Morgan, *AAPG Bull.* **56**, 203 (1972); *Geol. Soc. Am. Mem.* **132**, 7 (1972).
12. In some reconstructions [for example, (66)], hotspot tracks from the North American and other nearby plates are used to estimate the motion of a group of plates, including the African plate, relative to the hotspots.
13. P. Molnar and J. Stock, *Nature* **327**, 587 (1987).
14. J. A. Andrews, thesis, Princeton University (1975).
15. M. Kono, in vol. 55 of the *Initial Reports of the Deep Sea Drilling Project*, E. D. Jackson *et al.*, Eds. (1980), p. 737.
16. R. G. Gordon, *Geophys. J. R. Astron. Soc.* **70**, 129 (1982).
17. _____ and C. D. Cape, *Earth Planet. Sci. Lett.* **55**, 37 (1981).
18. J. Francheteau, C. G. A. Harrison, J. G. Sclater, M. L. Richards, *J. Geophys. Res.* **75**, 2035 (1970).
19. R. G. Gordon and A. Cox, *ibid.* **85**, 6534 (1980).
20. G. Suárez and P. Molnar, *ibid.*, p. 5257.
21. S. C. Solomon, N. H. Sleep, D. M. Jurdy, *ibid.* **82**, 203 (1977).
22. See, for example, D. W. Forsyth and S. Uyeda, *Geophys. J. R. Astron. Soc.* **43**, 163 (1975); (23); B. H. Hager and R. J. O'Connell, *J. Geophys. Res.* **86**, 4843 (1981); J. F. Harper, *Rev. Aquatic Sci.* **1**, 319 (1989).
23. R. G. Gordon, A. Cox, C. E. Harter, *Nature* **274**, 752 (1978).
24. D. M. Jurdy and R. G. Gordon, *J. Geophys. Res.* **89**, 9927 (1984).
25. R. G. Gordon and D. M. Jurdy, *ibid.* **91**, 12389 (1986).
26. P. Molnar, T. Atwater, J. Mamerickx, S. M. Smith, *Geophys. J. R. Astron. Soc.* **40**, 383 (1975).
27. D. M. Jurdy, *Geology* **6**, 469 (1978).
28. J. Stock and P. Molnar, *Nature* **325**, 495 (1987).
29. G. D. Acton and R. G. Gordon, in preparation.
30. The skewness is the wave number-independent phase angle that describes the shape of a magnetic anomaly attributable to magnetic-polarity reversals recorded in the shallow oceanic lithosphere during sea-floor spreading [H. Schouten and K. McCamy, *J. Geophys. Res.* **77**, 7089 (1972); R. Blakely and A. Cox, *ibid.*, p. 4339].
31. The uncertainties of these data are assessed in detail in (29).
32. G. D. Acton and R. G. Gordon, *J. Geophys. Res.* **94**, 17713 (1989).
33. We specify the uncertainties in rotations in terms of the angular standard errors associated with the three orthogonal directions found by diagonalization of a covariance matrix [D. M. Jurdy and M. Stefanick, *J. Geophys. Res.* **92**, 6310 (1987); T. Chang, *J. Am. Stat. Assoc.* **83**, 1178 (1988); T. Chang, J. Stock, P. Molnar, *Geophys. J. Int.* **101**, 649 (1990); P. R. Shaw and S. C. Cande, *J. Geophys. Res.* **95**, 2625 (1990); (48)], if these parameters were available. The directions are specified by the eigenvectors of the covariance matrix that specifies the uncertainties in the rotation; the angular standard errors are the square roots of the corresponding eigenvalues. If this covariance matrix was unavailable, as was true for most plate reconstructions, we approximated the errors by partial uncertainty rotations about three orthogonal axes defined by the paleogeometry of the plate and the location of a stage pole of rotation [J. M. Stock and P. Molnar, *Geology* **11**, 697 (1983); (67); J. Stock and P. Molnar, *Tectonics* **7**, 1339 (1988)].

34. The size of the uncertainty that accumulates through any one of the reconstruction links increases with the angular standard errors or the partial uncertainty rotation angles and with the sine of the angular distance between each paleomagnetic pole and each eigenvector or partial uncertainty rotation pole [(67); R. G. Gordon and G. D. Acton, in preparation]. Published reconstructions and reconstruction uncertainties are only available for specific ages when certain key magnetic lineations were created at sea-floor spreading centers. For ages between these, we used interpolated reconstructions and assumed that the reconstruction uncertainty was the same as that for the published reconstruction closest in age to the interpolated reconstruction. This simplification surely underestimated the real uncertainty. We also neglected the effect of the uncertainties in the age of paleomagnetic poles. Both of these effects increased the dispersion of the reconstructed non-Pacific paleomagnetic poles. Whenever a combination of reconstructed paleomagnetic poles gave a value of reduced chi square exceeding one, however, we rescaled errors upward to shrink reduced chi square to one. Therefore, extra dispersion caused by neglect of these two sources of error was in some cases incorporated into our rescaled error estimates.
35. The 26-Ma Pacific pole differs at the 5% significance level (that is, 95% confidence level) from two of four coeval poles, the 39-Ma Pacific pole differs from three of four coeval poles, the 58-Ma Pacific pole differs from five of eight coeval poles, and the 65-Ma Pacific pole differs from five of six coeval poles (Fig. 4).
36. All limits given herein are 95% confidence limits unless otherwise stated. The coeval mean reconstructed poles used for this calculation are not the same as those shown in Fig. 3, in which the mean reconstructed poles come from nonoverlapping data sets. To match the age of the Pacific poles as closely as possible, we introduced some overlap between sets of poles used to determine each mean reconstructed pole. The 27-Ma mean reconstructed pole was determined from non-Pacific poles with ages of 25, 26, 27, and 30 Ma. The 39-Ma mean pole was determined from these same 27- and 30-Ma non-Pacific poles plus non-Pacific poles with ages of 40, 49, and 49 Ma. The 56-Ma mean pole was determined from poles with ages of 53, 53, 55, 57, 60, and 60 Ma. The 64-Ma mean pole was determined from these two 60-Ma non-Pacific poles plus non-Pacific poles with ages of 63, 65, 65, and 73 Ma.
37. See, for example, (68); P. Bryan and R. G. Gordon, *J. Geophys. Res.* **91**, 462 (1986). For a trivial example, consider estimates of the distance between a point and itself. If calculated from the distance between two independent estimates of its location, the estimated distance is always greater than zero although the true distance is of course zero. Moreover, the size of the bias increases with increasing uncertainty in either estimate of the location of the point.
38. In the simulations, the size of the errors and the orientation of the error ellipses relative to the great circle connecting the poles were held at their estimated values. The angular distance between the poles was varied until three key distances were located: (i) the distance that produced a simulated average angular distance equal to the distance between estimated poles, (ii) the distance for which only 2.5% of the simulations gave distances equaling or exceeding the distance between estimated poles, and (iii) the distance for which only 2.5% of the simulations gave distances equal to or less than the distance between estimated poles. Thus, the interval between (ii) and (iii) is a 95% confidence interval. For the comparison of the poles at 26 Ma, an assumed angular distance of zero produced a distance equal to or in excess of the distance between observed poles in 6.5% of the cases; no value of angular distance gave distances equal to or in excess of the observed distance in as few as 2.5% of the simulations. In other words, the unbiased distance differs insignificantly from zero. For this case, a two-sided 95% confidence limit is impossible. The limits we quote correspond to one-sided significance levels of 6.5% for the lower bound and of 2.5% for the upper bound. Thus, the quoted interval corresponds to either a 91.0% or 97.5% confidence interval, depending on whether zero distance is included in the interval.
39. Compare with the discussion in (68), p. 59.
40. D. H. Coupland and R. Van der Voo, *J. Geophys. Res.* **85**, 3529 (1980); R. A. Livermore, F. J. Vine, A. G. Smith, *Geophys. J. R. Astron. Soc.* **79**, 939 (1984); D. A. Schneider and D. V. Kent, *J. Geophys. Res.* **93**, 11621 (1988).
41. Of the 22 comparisons of Pacific with reconstructed non-Pacific poles, 10 still differ at the 95% confidence level, and 4 of the 22 differ at the 95% confidence level.
42. Of the 22 comparisons of Pacific with reconstructed non-Pacific poles, seven still differ at the 95% confidence level, and 3 of the 22 differ at the 99% confidence level.
43. The motion of Africa over the Tristan da Cunha hotspot is presumed to have created the Walvis Ridge in the South Atlantic.
44. For example, (15–17) and many later papers.
45. In a reference frame in which the Pacific plate is held fixed.
46. These are the discrepancies found with use of the rotations of Morgan (66). These uncertainties are those induced by the uncertainties in the individual reconstructed points plus nominal ± 100 -km ($= \pm 1\sigma$) uncertainties in the past locations of the Hawaiian hotspot in directions both parallel and perpendicular to the Hawaiian-Emperor chain. We calculated these differences and uncertainties using rotation parameters, including those of Morgan (66) for the motion of the African plate relative to the hotspots, that are similar to those used by Molnar and Stock (13). Smaller differences are found if O'Connor and Duncan's (69) rotations of Africa relative to the hotspots are used instead of those of Morgan (66). Use of different rotations of Africa relative to the hotspots has no effect, of course, on the paleomagnetic discrepancy, discussed below.
47. Because our initial estimates of reduced chi square were usually near one and because we rescaled errors upward to shrink reduced chi square to one when it was larger, we believe but cannot prove that our error budget has been conservative enough to include almost any error systematic to only one pole or plate. Moreover, many of the systematic errors that we can imagine occurring in paleomagnetic data should be minimized because the data include paleopoles and paleolatitudes from many different rock types that are distributed widely over Earth's surface. Although we can exclude a consistent, persistent axial quadrupole component larger than $4 \pm 4\%$ of the dipole, we cannot exclude more complicated paleofields. Such an explanation is untestable, however, and would require that the paleomagnetic field from 25 to 73 Ma differed from the recent field in the correct sense and in just the right amount to explain the observed discrepancies.
48. J.-Y. Royer and T. Chang, *J. Geophys. Res.* **96**, 11779 (1991).
49. S. C. Cande, J. Stock, C. A. Raymond, W. F. Haxby, *Eos* **73** (October suppl.), 507 (abstr.) (1992).
50. C. DeMets, R. G. Gordon, D. F. Argus, S. Stein, *Geophys. J. Int.* **101**, 425 (1990).
51. C. DeMets, R. G. Gordon, P. Vogt, *ibid.*, in press.
52. D. F. Argus and R. G. Gordon, in preparation.
53. P. G. Fitzgerald, M. Sandiford, P. J. Barrett, A. J. W. Gleadow, *Earth Planet. Sci. Lett.* **81**, 67 (1986); A. J. W. Gleadow and P. G. Fitzgerald, *ibid.* **82**, 1 (1987).
54. T. A. Stern and U. S. ten Brink, *J. Geophys. Res.* **94**, 10315 (1989).
55. U. S. ten Brink, S. Bannister, B. C. Beaucloux, T. A. Stern, *Science* **261**, 45 (1993).
56. D. K. Blackman, R. P. Von Herzen, L. A. Lawver, in *The Antarctic Continental Margin: Geology and Geophysics of the Western Ross Sea*, A. K. Cooper and F. J. Davey, Eds. (Earth Sci. Ser., vol. 5B, Circum-Pacific Council for Energy and Mineral Resources, Houston, TX, 1987), pp. 179–190.
57. W. Hamilton, *Tectonophysics* **4**, 555 (1967); C. R. Bentley, in *Antarctic Earth Science*, R. L. Oliver, P. R. James, J. B. Jago, Eds. (Cambridge Univ. Press, Cambridge, 1983), pp. 491–497.
58. R. G. Allis, *Geology* **9**, 303 (1981); P. J. J. Kamp, *Tectonophysics* **121**, 225 (1986); *Geol. Soc. Am. Bull.* **97**, 255 (1986).
59. P. J. J. Kamp and P. G. Fitzgerald, *Geology* **15**, 694 (1987).
60. C. L. Mayes, L. A. Lawver, D. T. Sandwell, *J. Geophys. Res.* **95**, 8543 (1990).
61. D. C. Engebretson, A. Cox, R. G. Gordon, *ibid.* **89**, 10291 (1984); J. W. C. Rosa and P. Molnar, *ibid.* **93**, 2997 (1988).
62. K. E. Petronotis, R. G. Gordon, G. D. Acton, *Geophys. J. Int.*, in press.
63. E. Farrar and J. M. Dixon [*Earth Planet. Sci. Lett.* **53**, 307 (1981)] proposed that the present Pacific plate was two distinct plates separated before 43 Ma by a boundary in the central Pacific that they termed the "Emperor fracture zone." R. G. Gordon [*Geophys. Res. Lett.* **9**, 1283 (1982)] showed, however, that their proposed model was inconsistent with available paleomagnetic data.
64. S. C. Cande, E. M. Herron, B. R. Hall, *Earth Planet. Sci. Lett.* **57**, 63 (1982).
65. Before the existence of the Bellingshausen plate had been recognized by Stock and Molnar (28), Cande *et al.* (64) interpreted the Aluk plate as having lain between the Farallon plate and the Antarctic (not Bellingshausen) plate. Herein we incorporate the revised history of the southwest Pacific of (28) in describing the results of (64).
66. W. J. Morgan, *Tectonophysics* **94**, 123 (1983).
67. P. Molnar and J. M. Stock, *J. Geophys. Res.* **90**, 12537 (1985).
68. A. Cox and R. G. Gordon, *Rev. Geophys. Space Phys.* **22**, 47 (1984).
69. J. M. O'Connor and R. A. Duncan, *J. Geophys. Res.* **95**, 17475 (1990).
70. The largest confidence limit on the poles from the rest of the globe is for the pole at 46 Ma. It would have been much smaller if we had omitted the 49-Ma pole from North America, which we suspect of being unrepresentative of stable North America.
71. D. A. Clague and G. B. Dalrymple, *U.S. Geol. Surv. Prof. Pap.* **1350** (1987), p. 5.
72. J.-Y. Royer and D. T. Sandwell, *J. Geophys. Res.* **94**, 13755 (1989).
73. J. Stock and P. Molnar, *ibid.* **87**, 4697 (1982).
74. G. D. Acton and R. G. Gordon, *Geophys. J. Int.* **106**, 407 (1991).
75. This work has been supported by the National Science Foundation (EAR-9005679, OCE-9019318, and OCE-9116193), the Woods Hole Oceanographic Institution's Postdoctoral Scholar program, and the Caswell Silver Research Foundation.